Vapor Pressure of Normal Paraffins Ethane Through *n*-Decane from Their Triple Points to About 10 Mm Hg

Grant F. Carruth[1] **and Riki Kobayashi**[2]
Rice University, Chemical Engineering Department, Houston, Tex. 77001

Experimental determinations of the vapor pressures of the normal paraffins ethane through *n*-decane are reported from their respective triple points to about 10 mm of Hg. The steady-state gas-saturation technique and apparatus used for the measurements are described.

An accurate knowledge of the vapor pressures of hydrocarbons from the critical to the triple point is essential for both theoretical and applied end uses. Vapor pressures are adequately known for most hydrocarbons above 10 mm of Hg (*61, 68, 72*) but very few data, which are needed for many investigations into the fundamental nature of matter, exist below this value. Low-temperature extensions of the principle of corresponding states require such data (*34*). Studies in low-temperature phase equilibrium require accurate vapor pressure data (*8, 74*), as do further developments of low-temperature liquid-phase fugacity correlations (*9*). Studies of molecular interactions between unlike molecules through use of the enhancement factor (*25, 28, 30, 65*) require vapor pressure data.

In addition, reliable vapor pressure data are needed for petrochemical and other industrial concerns which utilize progressively more cryogenic processing technology. Low-temperature fractionation is useful in the separation and identification of products formed in hydrocarbon reaction kinetics. Efficient fractionation requires a knowledge of the vapor pressure of the constituents. Increased liquefied natural gas operations emphasize the need for basic knowledge of the principal constituents of natural gases down to the respective triple points.

General Techniques for Measurement of Vapor Pressures

Excellent summaries of the various methods for determining vapor pressures are given by Partington (*49*), Nesmeyanov (*47*), Weissberger (*73*), and Hála et al. (*24*). The main methods are discussed briefly below.

In the static method the equilibrium pressure in a thermostated chamber is determined, generally with a total-pressure device such as a liquid-filled manometer, gage, Bourdon tube gage, hot wire or radiation manometer, dead weight gage, vapor ionization gage, mass spectrometer, weight of the vapor contained in a volume, measurement of the deflections of a diaphragm, Knudsen's "absolute" manometer (*32*), and the McLeod gage. The latter two are the only truly "absolute" gages for very low pressure, although the McLeod gage is generally unsuitable for vapor pressure determinations (*17, 21*).

Static methods are not suited for low pressures and/or low temperatures, for several reasons. Wall adsorption at cryogenic temperatures can cause serious errors (*66*). For precise results at low total pressures, high-purity test samples are required. If the measurement device is not close to the same temperature as the equilibrated vapor, the thermomolecular pressure effect (thermal transpiration) exists (*50*) and must be taken into account (*38*). Correction for this effect requires a rather large amount of data on each gas studied (*37*). Careful calibration with respect to pressure and the particular compound studied is required for most of the above measuring devices. Devices involving displacement of a liquid interface are exceptions, although problems of cleaniness of the confining wall are often significant (*26*).

Absolute accuracies of most of the above vacuum-measuring techniques are seldom better than ±10% and frequently worse (*35*). With specialized techniques and great care, accuracies of a few percent have been claimed (*1, 17, 35, 66*).

A second general method is the dynamic method (or boiling point) (*24*), in which the sample is varied either isobarically or isothermally until ebullition occurs. Some major shortcomings include precise detection of incipient boiling and prevention of superheating. This technique has greatest utility in measuring relatively higher vapor pressures.

The effusion method (*31*) has been used extensively for studies of metals and other solids and also for high-molecular-weight hydrocarbons (*48*). The rate of effusion of equilibrated vapor into a vacuum through a small orifice is determined. The mean free path must be at least an order of magnitude larger than the dimensions of the orifice, which restricts application to less than 0.1 mm of Hg. Major problems are proper equipment design and construction, accurate determination of the rate of vapor effusion, and inadequate knowledge of the accommodation (evaporation) coefficient (*47, 49*) required for calculation of the pressure.

Another frequently employed century-old (*57*) method is the gas saturation (also referred to as transport, entrainment, flow) technique. The method is especially suitable for low vapor pressures less than 1 mm of Hg, although it has been used for vapor pressures up to several hundred millimeters of Hg (*57, 73*). A nonreactive insoluble gas is passed through the test sample at conditions which will yield complete saturation, and the rate of vapor removal or the saturated vapor concentration in the gas is determined. In principle, the method is free of serious errors and results can readily be employed with results obtained by other means (*24, 49*). Much of the criticism of the method has been due to assumptions made during calculations of the vapor pressure and the fact that the inherent simplicity of the method tends to induce one to take unjustified shortcuts in the experimental technique. Gerry and Gillespie (*22*) present an excellent review of the calculational procedures used.

Choice of Analytical Technique

The gas saturation method employing a flame ionization detector for gas mixture analysis was chosen for the following reasons: Adsorption effects can be minimized if sufficient time is allowed for all variables to reach a steady state. Expansion, compression, or other manipulation of the equilibrated gas mixture is unnecessary, as the mixture is conveyed rapidly and continually to the gas analyzer. The effect of volatile impurities is small, since the partial pressure of the sample vapor is measured

[1] *Present address, Research and Development Laboratory, E. I. du Pont de Nemours and Co., Old Hickory, Tenn. 37138.*
[2] *To whom correspondence should be addressed.*

rather than its total pressure. The thermomolecular pressure effect is eliminated. The method is relatively simple and the important variables are measurable to a high degree of precision. The property actually measured is the concentration of vapor molecules in equilibrium with the liquid, a fundamental quantity, since at a few microns of Hg "pressure" the mean free path is of the order of centimeters. [Consequently, the classical concept of "pressure" becomes somewhat ambiguous as pressure has meaning only when statistically averaged over a great number of molecules (*10, 36*). However, the idea of "number density" remains a well-defined concept at all pressures, so that the measurement of number density is highly desirable.] Some insight should arise in unlike molecular interactions, as the common carrier gases differ considerably in molecular size from the hydrocarbons studied.

The flame ionization detector was chosen for gas mixture analysis. It has high sensitivity to hydrocarbons and low response to common pollutants such as water vapor, CO_2, and CO, and to common nonhydrogen-containing carrier gases such as He, Ar, and N_2 (*12*). It has a wide dynamic range (*14, 23, 43*), generally with a wide linear range, and can detect very small concentrations. There is no strong dependence on design or operational parameters, such as interelectrode distance, polarizing potential, electrode configuration (if the electrode is not directly heated by the flame, which can cause thermionic emission), small flame temperature fluctuations, and small variations in hydrogen, air, or carrier gas flowrates.

For highest precision, the flame ionization detector (FID) should be calibrated for the materials being studied, although the signal response is approximately proportional to the flow of carbon atoms to the detector per unit time.

A flow method was chosen for calibration of the FID (*6*) and a special micropump was designed and built for this purpose (*5, 62*). A flow calibration method minimizes wall adsorption, which frequently can cause serious errors in other calibration techniques, such as exponential dilution (*29, 40*), direct injection (*43, 45*), and diffusion cell procedures (*2, 29*). Additionally, concentration changes can be made rapidly. The method is usable from very low up to large concentrations. The flow method, when applied over wide ranges of concentration, also facilitates the determination of relative response factors for compounds.

Helium was chosen as the carrier gas because it has a very low solubility in hydrocarbons, especially at low temperatures; it can be obtained commercially with high purity (<0.5 ppm hydrocarbons); it has a very low response in a flame ionization detector; and its volumetric properties are accurately known over the temperature range of interest.

Theoretical Development

Calculation of vapor pressures. Several methods (*4, 22, 41, 47, 49*) have been employed for extracting vapor pressures from the data of the gas saturation method. The method adopted for use here was to measure Py at several total pressures and extrapolate a plot of log Py vs. P to P^s or, by assuming $P - P^s \cong P$, to extrapolate the plot to $P = 0$. This method, while commonly employed empirically, can be derived from thermodynamic considerations. For a univariant equilibrium between a pure substance in the vapor phase and the corresponding condensed pure phase, the vapor pressure is a function of temperature only. Assume that an inert noncondensable gas is introduced into this system until the total pressure becomes P and the new system attains phase equilibrium. Then for the condensable component 2 in the vapor phase, one may write (*54–56*)

$$f_2^v = \phi_2^v y_2 P \tag{1}$$

For the condensable component 2 in the condensed phase, one writes

$$f_2^c = \gamma_2 x_2 f_2^{0c} \exp \int_0^P \frac{\bar{V}_2^c}{(RT)}\, dP \tag{2}$$

where

$$f_2^{0c} = P_2^s \phi_2^s \exp \int_{P_2^s}^0 \frac{V_2^c}{(RT)}\, dP \tag{3}$$

In the present investigation, where the condensed phase is well removed from its critical conditions and the pressure is low, one may assume that $V_2^c \cong \bar{V}_2^c$, so that

$$f_2^c = \gamma_2 x_2 P_2^s \phi_2^s \exp \int_{P_2^s}^P V_2^c/(RT)\, dP \tag{4}$$

Also, one may assume that the condensed phase molar volume is not a function of pressure. Making this substitution and equating the fugacities of component 2 in the vapor and condensed phases at equilibrium and rearranging give

$$\phi_2^v y_2 P = \gamma_2 x_2 P_2^s \phi_2^s \exp \int_{P_2^s}^P V_2^c/(RT)\, dP \tag{5}$$

or, from the definition of the fugacity coefficient (*51*),

$$\ln \phi_i = 1/(RT) \int_0^P \left[\left(\frac{\partial V}{\partial n_i} \right)_{T,P,n_j} - (RT)/P \right] dP \tag{6}$$

we have

$$RT \ln \frac{Py_2}{\gamma_2 x_2 P_2^s} = - \int_0^P \left[\left(\frac{\partial V}{\partial n_2} \right)_{T,P,n_1} - RT/P \right] dP + \int_0^{P_2^s} (V_2/n_2 - RT/P)\, dP + \int_{P_2^s}^P V_2^c\, dP \tag{7}$$

The first integral is evaluated for the vapor phase mixture, the second for the pure vapor component, and the third for the condensed component. This expression includes the lowering of vapor pressure due to solubility of the gas in the liquid phase (Raoult's law), the increase in vapor pressure due to the Poynting correction, and expressions for the vapor phase nonideality.

If it can be justifiably assumed that the inert gas is insoluble or very sparingly soluble in the condensed phase, then $x_2 = 1$ for the pure condensed phase. The activity coefficient of component 2 in the condensed phase also approaches unity due to the conventional normalization of liquid phase activity coefficients. Letting the enhancement factor, ϵ, be defined by $\epsilon = Py_2/P_2^s$, then

$$RT \ln \epsilon = RT \ln (Py_2/P_2^s) = - \int_0^P \left[\left(\frac{\partial V}{\partial n_2} \right)_{T,P,n_1} - \frac{RT}{P} \right] dP + \int_0^{P_2^s} \left(\frac{V_2}{n_2} - \frac{RT}{P} \right) dP + \int_{P_2^s}^P V_2^c\, dP \tag{8}$$

This same result has been derived by Beattie (*3*), by Dokoupil et al. (*15*), who initially assumed that the inert gas was insoluble, and by Chiu and Canfield (*11*).

For practical use, an equation of state such as the Beattie-Bridgeman, Benedict-Webb-Rubin, or virial is required. Such equations have been used primarily to test various mixing rules for equation of state parameters (*30, 65*) and to estimate interaction virial coefficients, as done by Reuss and Beenakker (*59*), Ewald (*19*), and Chiu and Canfield (*11*), or to test solubility data against theoretical predictions (*15, 20, 60*).

If the virial equation, truncated after the third virial coefficient, and the conventional virial equation mixing rules are assumed, one obtains

$$RT \ln \frac{Py_2}{P_2^s} = V_2^c(P - P_2^s) + B_{22}P_2^s - (1 - y_1^2)B_{22}P + \frac{(C_{222} - B_{22}^2)(P_2^s)^2}{2RT} + (B_{11} - 2B_{12})y_1^2P + \frac{P^2}{2RT}[-3y_1^2C_{112} - 6y_1y_2C_{122} - 3y_2^2C_{222} + y_1^3(2C_{111} + 4B_{11}B_{12}) + y_1^2y_2(6C_{112} + 4B_{11}B_{22} + 8B_{12}^2) + y_1y_2^2(12B_{12}B_{22} + 6C_{122}) + y_2^3(4B_{22}^2 + 2C_{222}) - y_1^4(3B_{11}^2) - y_1^3y_2(12B_{11}B_{12}) - y_1^2y_2^2(6B_{11}B_{22} + 12B_{12}^2) - y_1y_2^3(12B_{12}B_{22}) - y_2^4(3B_{22}^2)] \quad (9)$$

For most of the range covered in this work, the simplification can be made that

$$y_2 \simeq 0 \qquad y_1 \simeq 1 \qquad x_2 \simeq 1 \qquad x_1 \simeq 0 \quad (10)$$

Then, if higher order pressure terms are neglected, the result is

$$RT \ln \frac{Py_2}{P_2^s} = V_2^l(P - P_2^s) + B_{22}P_2^s + (B_{11} - 2B_{12})P + \frac{(C_{222} - B_{22}^2)(P_2^s)^2}{2RT} \quad (11)$$

Use of other equations of state reported (*30, 60, 65*) yields a similar pressure dependence. If it is further assumed that $P \gg P_2^s$, the previously mentioned linear extrapolation of ln Py vs. total pressure P is obtained, with the intercept giving the vapor pressure. Thus,

$$\ln \frac{Py_2}{P_2^s} \simeq \frac{(V_2^l + B_{11} - 2B_{12})P}{RT} = (\text{Slope})(P) \quad (12)$$

This is the working equation for the calculation of the vapor pressures in this work. It was derived by making certain simplifications to a rigorous thermodynamic expression for phase equilibria. The assumptions are tabulated and discussed below.

The virial equation provides an accurate description of the vapor phase. This equation has been used frequently in related studies at higher pressures. With respect to the helium–hydrocarbon systems studied in this work, it is questionable that a hydrocarbon molecule ever reacts with only one helium molecule, because of the size disparity and the large number of helium molecules per hydrocarbon molecule at these low temperatures and low vapor pressures. A more definitive approach would involve some expression which relates vapor phase interaction coefficients as functions of say, density, and a "coordination number"—i.e., a measure of the number of helium molecules interacting with a hydrocarbon molecule during some statistical period of time. Such a development is still in an elementary state, although work along these lines is proceeding in this laboratory. Consequently, in this work the virial equation is used (for illustration) for want of a better expression because it appears to be fairly successful, especially when modifications are made to the conventional mixing rules (*28*). Of course, for purposes of this work, no commitment is required as pertains to the functional form of the term given by the slope of the ln Py vs. P curve.

The condensed phase is incompressible. This is an excellent assumption at the low temperatures and low total pressures employed in this work.

Terms of order P^2 or larger are negligible. This assumption is consistent with the approximation that the virial equation is accurate at the low total pressures used in this study.

The helium carrier gas is insoluble in the condensed phase. Very few solubility data exist for helium–hydrocarbon systems at low temperatures. Two general conclusions are obtainable from the available data: Helium solubility is very low in saturated hydrocarbons at low temperature and pressure, and helium solubility decreases with decreasing temperature. From solubility data for helium in propane (*63*) from −150° to 75°C and 200–3000 psia, in methane (*64*) from −85° to −180°C up to 2000 psia, and in ethane at 170K and 200 atm, it is reasonable to conclude that the solubility at 1 or 2 atm would be considerably less than 1%. No solubility data were found for helium in the heavier hydrocarbons. However, data given by Lannung (*33*), Stephen and Stephen (*67*), and Markham and Kobe (*42*) indicate that the solubility of helium in benzene and cyclohexane at room temperature is no greater than a few hundredths mole percent. Consequently, the assumption that helium is effectively insoluble in the hydrocarbon appears to be valid.

The mole fraction of helium in the vapor phase is assumed to be essentially unity. This effect was evaluated for ethane at a temperature giving a vapor pressure of 40 mm of Hg, since this was the highest pressure measured and since ethane would be most likely to be adequately described by the virial equation. The second virial coefficient of ethane was estimated by the correlation of Pitzer and Curl (*52*). The interaction virial coefficient, B_{12}, was estimated by standard techniques (*27, 58*). The difference between the vapor pressure computed by Equation 9 (with terms of order P^2 omitted) and the simplified Equation 12 was less than 0.4% for the condition tested. The difference should be less as the temperature is reduced and as the vapor pressure becomes smaller. The slopes, as determined by experimental data, are somewhat greater than those estimated by the above calculations, probably because of inadequacy of the mixing rules, of the virial equation, or other effects. This is consistent with observations of other investigators.

The vapor pressure can be neglected in the extrapolation of the simplified equation. This was tested at 40 mm of Hg, assuming the total pressure was 780 mm of Hg. A typical value of the slope as indicated by experimental data was used to show that the maximum error in vapor pressure due to extrapolating to $P = 0$ rather than $P = P^s$ was no more than 0.25%.

Experimental Details

Calibration curves were prepared for each compound by metering known rates of hydrocarbon into a steady flow of helium carrier gas and determining the hydrocarbon response in a flame ionization detector. Hydrocarbon was metered with a unique positive-displacement micro-

pump and transmission capable of delivering maximum and minimum flow rates of 0.36 to 8 × 10^{-8} cm^3/min, respectively. Mechanical details of the pump and transmission are discussed elsewhere (*5, 62*), as are detailed calibration procedures and results (*5, 6*). Pump temperature was measured and controlled to ±0.1°C and pump pressure was measured to +0.01 in. of Hg. Uncertainty in displaced volume was ±0.05%. The volumetric flow rate of the micropump, temperature of the pump, pressure of the pump, and the FID response were recorded. Since liquid density is accurately known in the temperature range used (*61*), the molar flowrate of hydrocarbon can be calculated. For ethane, propane, and butane, metered as vapors, the second virial coefficient (*18*) was used to calculate the compressibility factor. The molar flowrate of hydrocarbon was plotted vs. detector signal in log–log coordinates. Analytical curves then were fitted to the data by least-squares regression.

After calibration, hydrocarbon was discharged to the equilibrium apparatus shown schematically in Figure 1. Carrier gas was metered with a positive displacement pump and the pressure, temperature, and volumetric flowrate of the pump were recorded. The metered carrier gas was passed through a thermostated presaturator and then was bubbled through hydrocarbon contained in the thermostated equilibrium cell. The steady-state pressure and temperature of the cell were recorded, as was the resulting FID signal. Equilibrium values were recorded at three or four pressures for each isotherm. From the least-squares calibration curve, the flowrate of hydrocarbon was determined and the flow rate of helium was known from metering information. Consequently, the vapor concentration and thus the partial pressure of hydrocarbon were readily calculated. The saturated vapor pressure was extracted as described in the theoretical discussion.

Flame ionization detector. A Barber-Coleman flame ionization detector was used which employed a 1-cm diameter platinum ring as an ion collector. The ring was positioned 1 cm above the stainless steel burner tip and operated at ±240 V dc with respect to the grounded burner tip. The FID was operated at 116 ± 1°C. Matheson Co. hydrogen Zero gas (<1 ppm hydrocarbon) and air Zero gas (<2 ppm hydrocarbon) were used to supply the flame of the FID. A 1/16-in. capillary restrictor was attached just prior to injection of each supply gas into the FID. Adequate control was then attained by controlling the upstream pressure of the capillary restrictor with conventional pressure regulators. Optimum hydrogen and air flowrates were 26 and 386 cm^3/min, respectively.

The signal from the FID was measured with a Barber-Coleman electrometer capable of measuring 10^{-12} to 10^{-6} amp full scale. The standing current of the FID with an extinguished flame was 6 to 8 × 10^{-14} amp and, with the flame ignited, the standing current was 1.0 to 1.4 × 10^{-12} amp. With pure helium Zero gas flowing, the signal was typically 1.9 to 2.5 × 10^{-12} amp for flowrates of 12 cm^3/min. The helium baseline was very stable for a given run and was not significantly affected by small variations in the helium flowrates. Noise with pure helium carrier was about 5 × 10^{-15} amp.

Uncertainty in signal current measurements was 2–3% due to electrometer nonlinearities which had been reduced to this level by careful electronic calibration.

Carrier gas-metering pump. The helium carrier gas was metered with a 500-cc positive displacement plunger

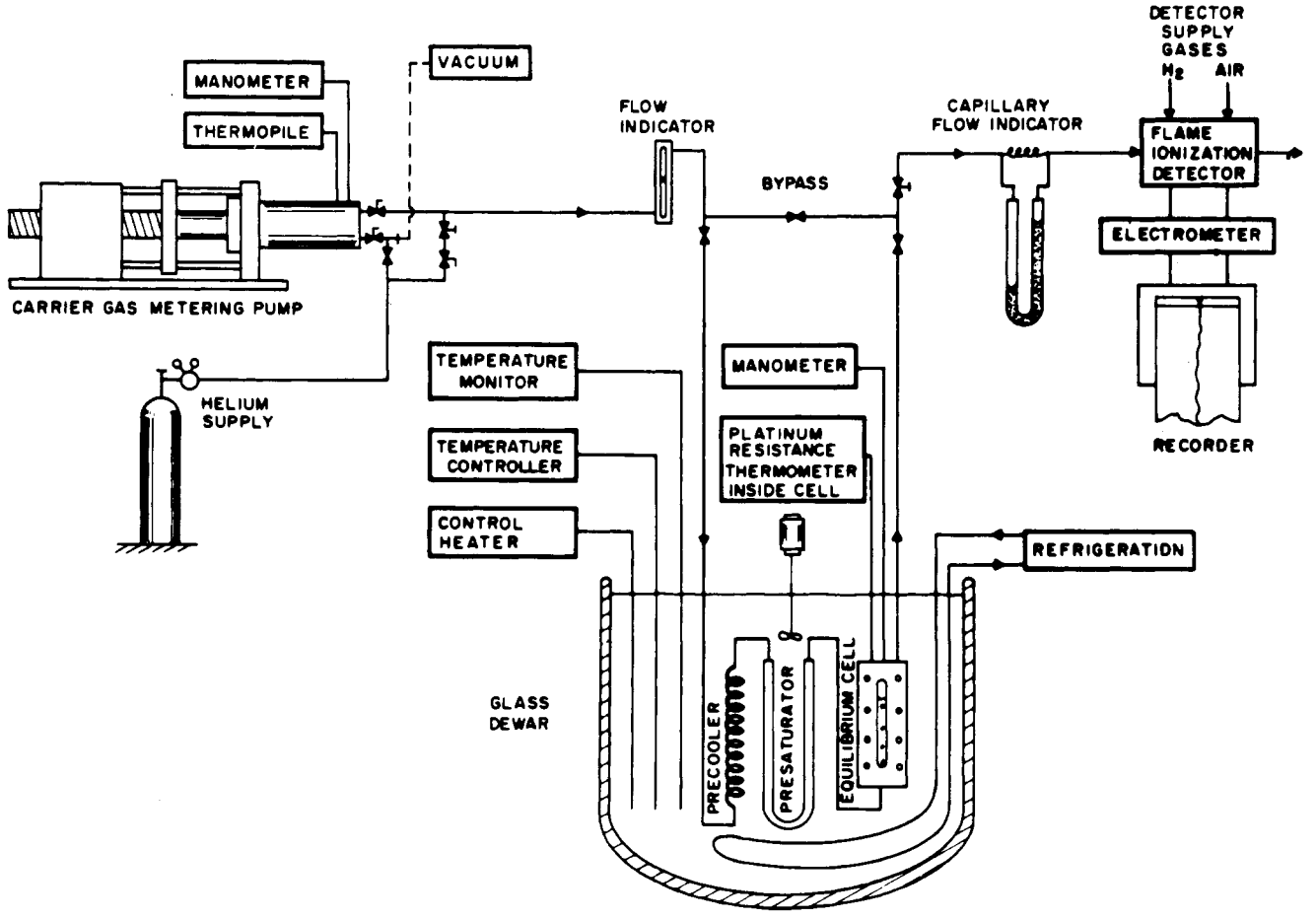

Figure 1. Isothermal gas saturation flow system used for vapor pressure measurement

pump with a maximum uncertainty of 0.018% in displaced volume. Pump pressure was measured to ±0.01 in. of Hg with a mercury manometer. The temperature of the metered gas was measured by a ten-junction Chromel-Constantan thermopile contained in a 1/8-in. od probe inserted directly into the pump cylinder. The thermopile was calibrated against a platinum resistance thermometer (PRT). The entire pump was enclosed in a thermostated chamber controlled to better than ±0.1°C. Overall uncertainty in molar flowrate of helium was ±0.07%.

Equilibrium apparatus. The entire equilibrium apparatus (Figure 1) was mounted under a rectangular horizontal plate supported at four corners by vertical angle iron braces, which in turn were braced at top and bottom by horizontal angle iron braces. An 8½-in. diameter by 20½-in. deep cylindrical glass Dewar was mounted in a metal box and located directly below the equilibrium apparatus. The Dewar was silvered except for a vertical strip at front and back. By means of a crank and cables, the Dewar could be raised to enclose the equilibrium apparatus completely. This arrangement is termed a Riki box. The lower box was fitted with a vertical slot in front and back and a fluorescent lamp in the back, so that the contents of the Dewar could be illuminated.

Above the Riki box was a hood equipped with a 250-cfm exhaust fan. A fireproof curtain with a zipper closure was hung from the hood to the floor. Room air entered at the bottom of the assembly, passed up around the unit, and exhausted with any vapor rising from the bath fluid.

The precooler consisted of a section of coiled 1/8-in. stainless steel tubing 10 ft long. The presaturator design selected was a section of 3/8-in. stainless steel tubing approximately 36 in. long, bent as required. This was loosely filled with 50- to 60-mesh acid-washed firebrick (Chromopak) on which was placed about 25 to 30 weight % of the hydrocarbon being tested.

Liquid hydrocarbon in the visual equilibrium cell was either charged in as a liquid at room temperature (*n*-pentane and heavier compounds) or condensed in at low temperature. The equilibrium cell consisted of a stainless steel cylinder 1½-in. ID × 9-in. high free space fitted with ¼-in. thick glass windows front and back. The window was provided to observe the freezing point as well as to determine that a steady bubbling rate of carrier gas was attained. From the bottom carrier gas passed through a thin stainless steel plate perforated to establish a steady bubbling rate. The cell was partially filled with 3-mm glass beads which dispersed the bubbles so that a slight motion in the liquid was induced. A vapor space above the liquid was followed by a section tightly packed with fine copper turnings to serve as an entrainment separator. A Nupro micrometer valve, near the cell exit but outside the cryostat, controlled the back pressure in the cell.

The saturated carrier gas was then conveyed to the FID through a heated line. This line was equipped with a capillary flowmeter to assist in setting the back pressure valve to give the same carrier gas flow at all pressures. Equilibrium cell pressure was measured to +0.01 inch of Hg.

The equilibrium cell temperature was measured with PRT inserted approximately 7 in. into a bore in the wall of the cell. Resistance values were determined with a Mueller bridge. The IPTS 48 scale was used.

A slight excess of refrigeration was balanced with a controlled heat input to give a cryostat temperature controlled to ±0.005°C generally and no worse than ±0.015°C at the lowest temperatures. A stirrer provided circulation of bath fluids. No temperature gradients greater than the precision of temperature control could be detected anywhere in the cryostat. Refrigeration was provided by circulating liquid nitrogen through the refrigeration coils.

Bath fluids were commercial isohexane for measurements on the *n*-pentane and heavier compounds, commercial isopentane for *n*-butane, and propane for the ethane and propane experiments. Special precautions (*5*) were taken in handling the propane bath fluid.

Results

Freezing points. The freezing points of the hydrocarbons were taken as the temperature at which a steady carrier gas flow could be maintained with both liquid and solid phases present, as determined by visual observation. All hydrocarbons subcooled several tenths °C before freezing. The freezing points reported in Table I, under approximately 1-atm helium pressure, were taken primarily as an indication of purity, although they differ from literature values (*61*) for pure compounds by only a few hundredths °C.

Vapor pressure data. Saturated vapor pressures were calculated by the method of least squares applied to the simplified model discussed in the theoretical section,

$$\ln \frac{P_y}{P^s} = (\text{slope})\ (P) \qquad (12)$$

where the slope of the line ln Py vs. $(P - P^s)$ with $P \gg P^s$ is a measure of the vapor phase nonideality.

Experimental vapor pressure data are tabulated for each compound in Table II. Attempts to take data at higher vapor pressures fell beyond the range of the experimental technique. The highest points (30 to 40 mm of Hg) occur at concentrations very near the saturation limit of the detector. In this very nonlinear range, a large change in concentration results in a relatively small change in detector signal. Thus, the uncertainty in concentration is much higher at the high concentrations. The gas saturation method is generally less satisfactory at pressures greater than 10 mm of Hg or so (*47, 73*), as the assumptions made in the thermodynamic analysis become less accurate.

Comparison with other data. The experimental data and other available data are plotted for comparison in Figures 2 to 10. The results of this study appear to join smoothly with the API 44 compilation for each compound.

Ethane (Figure 2). This work plus that of Tickner and Lossing (*70*), and Delaplace (*13*) primarily comprise the experimental measurements below 10 mm of Hg, although a few other measurements from 1–10 mm of Hg have been reported associated with higher vapor pres-

Table I. Freezing Points under 1 Atm Helium Pressure

Compound	Obsd. freezing point, °C	API 44 value (*61*)
Ethane	[a]	−183.26
Propane	[b]	−187.68
n-Butane	−138.34	−138.35
n-Pentane	−129.73	−129.72
n-Hexane	−95.36	−95.35
n-Heptane	−90.60	−90.61
n-Octane	−56.81	−56.79
n-Nonane	−53.59	−53.52
n-Decane	−29.71	−29.66

[a] Carrier gas flow stopped at −182.80°C but liquid ethane did not freeze. An impurity apparently froze over holes in perforated plate. [b] Not obtained, since detector signal for propane could not be distinguished from baseline below ~−179°C.

Table II. Vapor Pressure Data for Paraffin Hydrocarbons

Ethane		Propane	
T, K	P, mm Hg	T, K	P, mm Hg
91.34	1.16×10^{-2}	94.54	4.98×10^{-5}
93.70	2.05×10^{-2}	99.78	2.60×10^{-4}
96.24	3.74×10^{-2}	105.15	8.41×10^{-4}
100.70	9.86×10^{-2}	110.65	3.28×10^{-3}
105.60	0.248	117.42	1.28×10^{-2}
114.24	1.10	127.72	8.52×10^{-2}
120.38	2.74	134.15	0.232
129.81	9.36	143.74	0.909
135.77	18.4	155.72	3.96
140.55	30.6	162.45	7.87
144.14	42.8	173.58	23.7
		178.65	34.3

n-Butane		n-Pentane	
T, K	P, mm Hg	T, K	P, mm Hg
135.43	6.77×10^{-3}	143.61	6.07×10^{-4}
137.73	8.10×10^{-3}	150.51	2.02×10^{-3}
138.93	1.09×10^{-2}	157.28	5.75×10^{-3}
146.32	3.85×10^{-2}	164.41	1.95×10^{-2}
148.10	5.09×10^{-2}	179.60	0.144
154.84	0.138	189.41	0.427
159.79	0.242	205.96	2.14
171.43	0.945	218.97	6.95
184.09	3.65	227.21	13.0
194.65	9.31	242.29	25.5
196.71	11.5		
205.27	23.5		
209.28	28.3		
212.90	37.1		

n-Hexane		n-Heptane	
T, K	P, mm Hg	T, K	P, mm Hg
177.71	1.02×10^{-2}	185.30	2.16×10^{-3}
178.02	1.03×10^{-2}	192.74	6.50×10^{-3}

n-Hexane		n-Heptane	
T, K	P, mm Hg	T, K	P, mm Hg
181.45	1.70×10^{-2}	204.94	3.18×10^{-2}
184.22	2.41×10^{-2}	217.45	0.123
189.16	4.48×10^{-2}	231.04	0.431
197.21	0.102	245.20	1.47
211.90	0.481	259.15	4.46
219.86	0.962	274.16	12.5
238.31	4.92	285.07	22.4
248.24	9.48	295.61	38.1
258.76	19.2		
264.94	23.4		

n-Octane		n-Nonane	
T, K	P, mm Hg	T, K	P, mm Hg
216.60	1.80×10^{-2}	219.66	5.69×10^{-3}
218.51	2.06×10^{-2}	223.75	6.19×10^{-3}
223.23	3.30×10^{-2}	224.89	6.94×10^{-3}
230.42	7.28×10^{-2}	236.83	2.43×10^{-2}
238.07	0.151	245.70	5.90×10^{-2}
250.09	0.445	263.18	0.280
259.40	0.958	275.75	0.753
278.41	3.99	294.14	3.03
289.56	7.85	300.05	4.52
297.11	11.8	307.74	5.42

n-Decane	
T, K	P, mm Hg
243.50	1.29×10^{-2}
251.31	2.40×10^{-2}
254.47	3.44×10^{-2}
263.61	7.95×10^{-2}
277.50	0.249
289.89	0.649
304.60	1.40
310.60	1.54

sures. The vapor pressures of ethane from 20K to the normal boiling point (184.52K) have been calculated by Ziegler et al. (*76*) from a thermodynamic analysis. Data required consist of T_b and T_t, ΔH_v of vaporization at T_b, ΔH_f of fusion at T_t, heat capacity of the saturated condensed phase over the entire temperature range, molar volume of saturated condensed phase over the entire temperature range, molecular weight, second virial coefficient of the saturated vapor over the temperature range, and the temperatures and enthalpies of any other phase transitions occurring. Additionally, sufficient molecular structure and spectroscopic data are required for evaluation of $(H^\circ - H_o^\circ)$ and (S°) for the ideal gas at 1 atm by statistical mechanical techniques. If all input data are highly accurate, reliable vapor pressure values should be possible.

The results of this work agree very well with the calculations of Ziegler et al. (*76*), except at the lowest temperatures, as slightly more curvature is found in Ziegler's results. However, since Ziegler's values can be linearly fit within a maximum pressure error of about 2 to 3% between 20 mm of Hg and the triple point, the amount of curvature of log P vs. $1/T$ is small in the very low pressure range. Experimental measurements accurate to 2 to 3%, as in this work, cannot detect this degree of curvature.

Delaplace (*13*) reported no pressure units with his results. Baryes were assumed to be the proper unit, but the results of Delaplace still differ significantly from all other results, and the functional form of the results appears unusual.

Tickner and Lossing's smoothed data (*70*) deviate significantly both from this work and from Ziegler's calculations. Application of Liang's thermomolecular corrections (*38*) enhance this deviation. Tickner and Lossing claimed a precision of temperature control of ±0.3K (equivalent to a pressure error of about 8% at T_t and 4% at 10 mm of Hg). A mass spectrometer, employed for partial pressure measurement, was not linear in pressure above 40 μ of Hg; so above this pressure it was necessary to expand the equilibrated vapor into "suitable calibrated volumes" (*70*) to reduce the pressure to within the linear range. Their results plotted on an expanded scale join API 44 results at a rather sharp angle which is unlikely from physical considerations. It is this author's belief that Tickner and Lossing's results are somewhat low, probably in

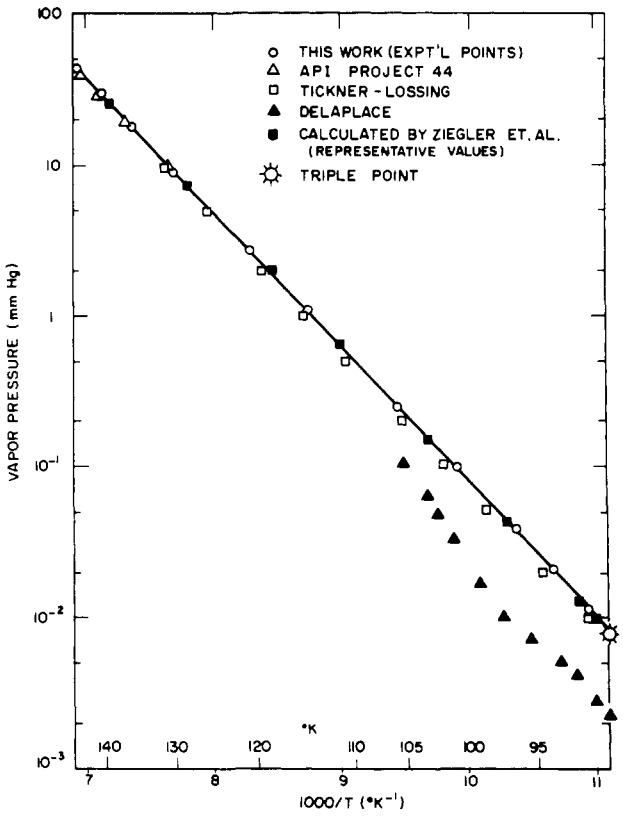

Figure 2. Comparison of ethane vapor pressure data with available literature values

part because of vessel wall adsorption of a portion of the equilibrated vapor during the expansion step, and also some uncertainty due to the precision of temperature measurement. Similar calculations by Ziegler et al. (*77*) for ethylene indicate that Tickner and Lossing's values are significantly lower, and for methane (*78*) show approximate agreement with Tickner and Lossing within the precision of their temperature control.

Propane (Figure 3). Agreement of Tickner and Lossing's values (*69, 70*) is satisfactory, but Delaplace's results (*13*) appear significantly different.

n-Butane (Figure 4). The data of this work for n-butane comprise two runs. No differences were noted between the data of the two runs. Delaplace's results (*13*) differ considerably and Tickner and Lossing's results (*69, 70*) are believed to be low for reasons discussed under the ethane section.

n-Pentane (Figure 5). Three points in the 1–10 mm of Hg range are taken from Messerley and Kennedy (*44*). Values from this work again are somewhat higher than Tickner and Lossing's smoothed results.

n-Hexane (Figure 6). Data points of Woringer (*75*) (reported in 1900) appear to be too high and actually lie higher than a linear extrapolation of API 44 (probably because of impurities). The data of Drucker et al. (*16*) agree rather well with this study but are slightly higher. Drucker et al. report a boiling point of their sample as 68.7°C at 740 mm of Hg as compared to 67.9°C at 740 mm in ref. *61*. This would indicate some volatile impurity which could explain the difference, as they measured total pressure and the work was reported in 1915 when purification techniques were not as well advanced as they are currently. Mündel's results (*46*) (reported in 1913) are also higher, probably because of volatile impurities.

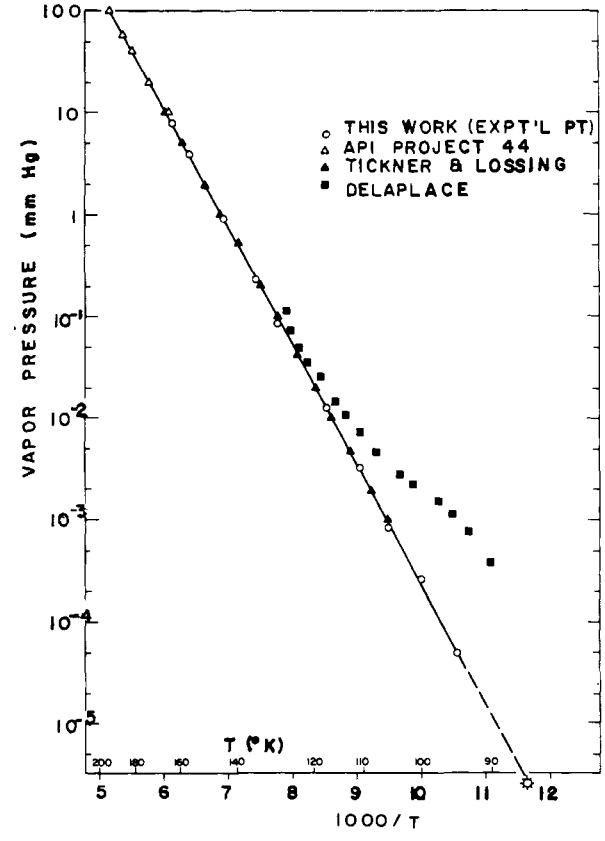

Figure 3. Comparison of propane vapor pressure data with available literature values

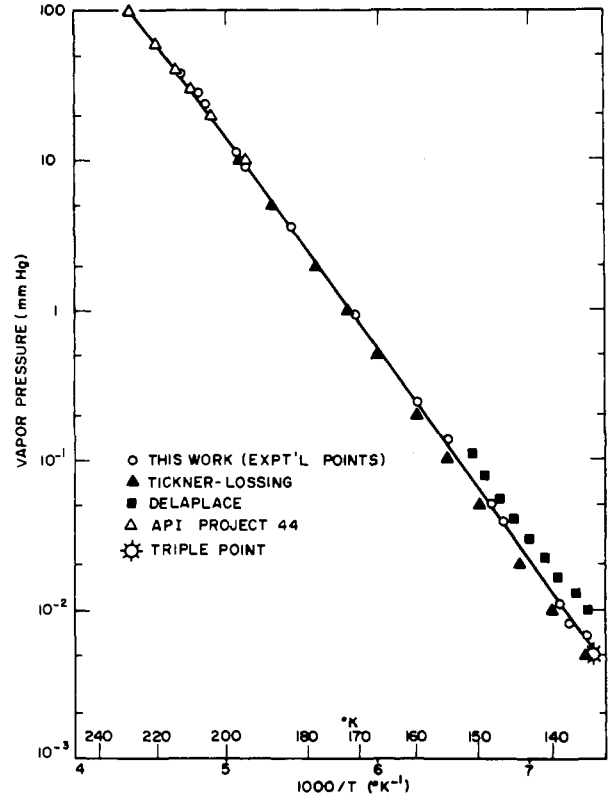

Figure 4. Comparison of *n*-butane vapor pressure data with available literature values

Table III. Constants of Vapor Pressure Smoothing Equation and Triple Point Pressure

Compound	A	B	T_t, K	$(T_t)r$	P_t, mm Hg
C_2H_6	18.0072	−2049.35	89.89	0.2943	8.30×10^{-3}
C_3H_8	18.6597	−2697.80	85.47	0.2311	2.49×10^{-6}
n-C_4H_{10}	18.8991	−3246.02	134.86	0.3171	5.68×10^{-3}
n-C_5H_{12}	19.7269[a]	−3899.67[a]	143.47	0.3055	5.79×10^{-4}[a]
n-C_6H_{14}	19.5553	−4292.80	177.83	0.3505	1.02×10^{-2}
n-C_7H_{16}	20.1590	−4852.65	182.55	0.3380	1.62×10^{-3}
n-C_8H_{18}	20.3621	−5294.36	216.37	0.3804	1.65×10^{-2}
n-C_9H_{20}	20.8468	−5811.26	219.65	0.3694	3.66×10^{-3}
n-$C_{10}H_{22}$	20.8865	−6170.32	243.50	0.3943	1.16×10^{-2}

Smoothed vapor pressure equation. $\ln P = A + B/T$, T in K, P in mm Hg

[a] Based on reprocessed data and indications from generalized correlation, following values are recommended:

$A = 19.7269$ $B = -3883.66$ $P_t = 6.47 \times 10^{-4}$ mm Hg

n-Heptane (Figure 7). Mündel's (*46*) values are somewhat higher than those of this work, probably because of impurities.

n-Octane (Figure 8). Woringer's results (*75*) are appreciably higher than any of the other data. The results of Mündel (*46*) and Linder (*39*) agree within a few percent and are higher than those of this work, possibly because of impurities. The data of Young, as reported by Timmermans (*71*), agree closely with this work.

n-Nonane (Figure 9). No results were found for comparison with this work below 10 mm of Hg.

n-Decane (Figure 10). Woringer's results (*75*) are considerably higher than those of this work. Linder's results (*39*) are slightly higher, probably because of some impurities.

The data were used to calculate liquid fugacity coefficients and entropies and enthalpies of vaporization at low temperatures. The data were used to extend the three-parameter (P_r, T_r, ω) corresponding states correlation proposed by Pitzer and Curl (*51, 52*) and Pitzer et al. (*53*) to the triple point of normal fluids with good accuracy. Thus, vapor pressures, enthalpies and entropies of vaporization, and liquid fugacity coefficients for normal fluids can now be predicted accurately from the triple point to the critical point. Detailed discussion of the correlation as well as comparison of the data with other generalized correlations is found elsewhere (*5, 7*). The experimental vapor pressure data are well represented by the Clausius-Clapeyron equation with constants as given in Table III. Ziegler et al.'s (*76*) idealized calculations of

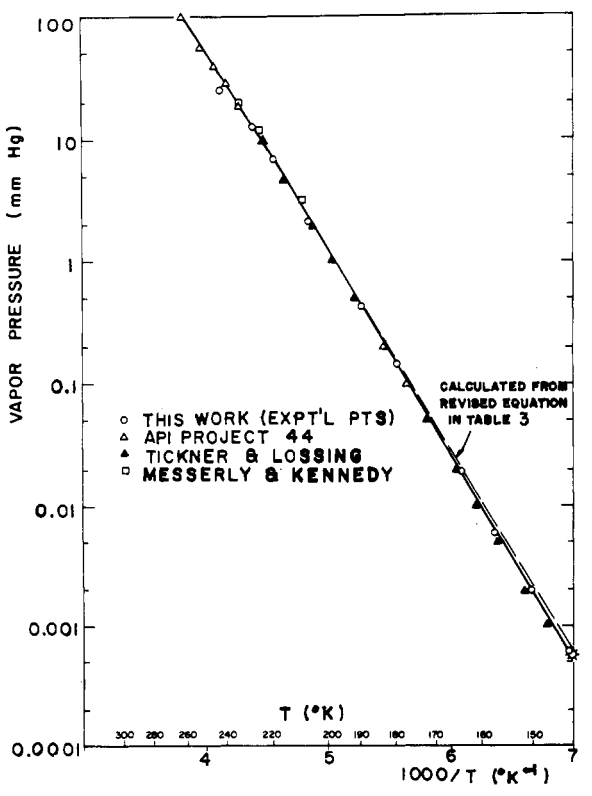

Figure 5. Comparison of *n*-pentane vapor pressure data with available literature values

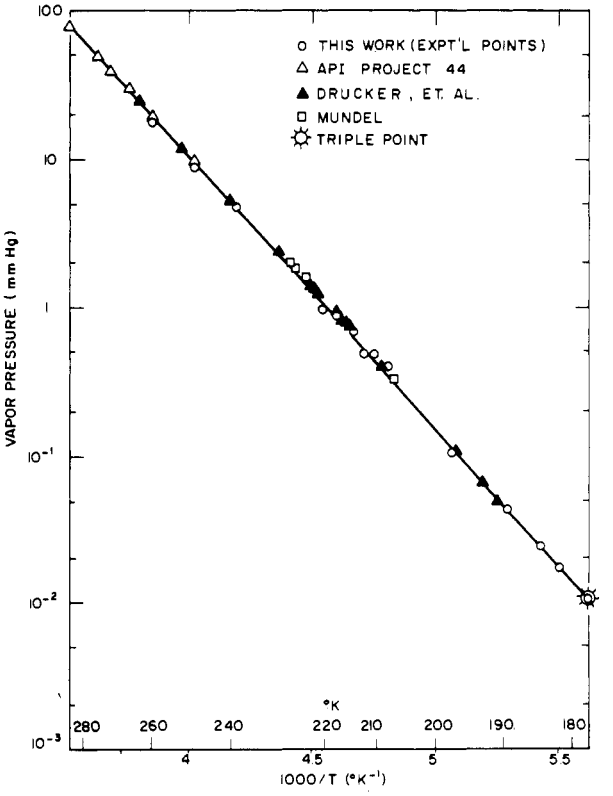

Figure 6. Comparison of *n*-hexane vapor pressure data with available literature values

the vapor pressure of ethane can be fitted to a straight line within 2 to 3% below 20 mm of Hg, which is consistent with the experimental accuracy of this work; and, while Tickner and Lossing (*70*) reported only smoothed results, their results lie on a straight line, leading to the inference that the original data were sufficiently linear to substantiate the linear smoothing which they employed. Within the experimental accuracy of this work, use of the linear smoothing equation appears justified.

Several *n*-pentane points deviate from the corresponding states correlation by a substantial amount. This is not totally unexpected, as more experimental difficulties were encountered on this run than on any other. This run was the second compound measured and the first one below −90°C. Improved experimental techniques were evolved principally in response to difficulties encountered in this run. It is this author's opinion that the original *n*-pentane points at 157.28, 164.41, 179.60, and 189.41K exceed the expected experimental error for the bulk of this work for some nontraceable reason, and that the low-temperature vapor pressure is given more reliably by the revised constants of Table III. This opinion is based upon the assumption that there is no reason for believing that *n*-pentane should not fit an acentric factor correlation (*5, 7*) which appears to fit the other *n*-paraffins well. Partial justification for this opinion arises because two points were rerun after the correlation was completed. These were higher than the original data, which is the direction expected from the use of the derived correlation.

Analysis of Errors

The ultimate accuracy of the results of this investigation is dependent upon (1) the validity of the thermodynamic model applied to the data, (2) the accuracy of the FID calibration, (3) the precision of temperature, pressure, volume, and vapor concentration control and/or measurement, (4) the requirement that the effluent gas mixture be completely saturated with the hydrocarbon vapor, and (5) other items, including the degree of solubility of helium in the hydrocarbon, possible entrainment, purity of the test sample, possible effect of the Knudsen thermomolecular effect, and avoidance of leaks in the apparatus.

Item 1 has been discussed previously. Experiments were conducted which showed that item 4 was satisfied. Purity of each compound studied is given in Table IV. The Knudsen thermomolecular effect does not occur because of the relatively high total pressures employed. The equipment was designed to eliminate possible entrainment as a source of error. Extensive testing was done to find and correct apparatus leaks. Items 2 and 3 are basi-

Table IV. Purity of Materials Used

Compound	Purity, mol %
Ethane	99.99
Propane	99.99
n-Butane	99.93
n-Pentane	99.90
n-Hexane	99.95
n-Heptane	99.92
n-Octane	99.85
n-Nonane	99.68
n-Decane	99.85
	Hydrocarbons, ppm
Helium Zero gas	<0.5
Hydrogen Zero gas	<1
Air Zero gas	<2

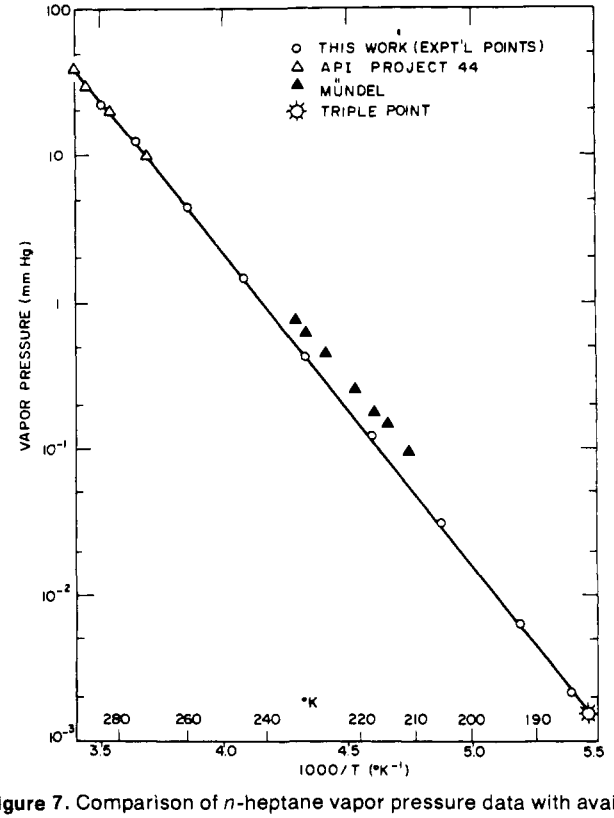

Figure 7. Comparison of *n*-heptane vapor pressure data with available literature values

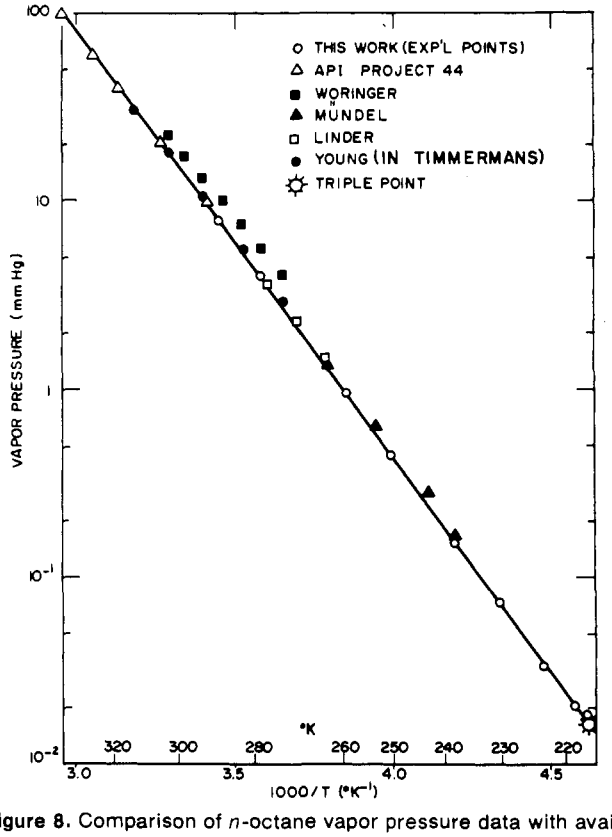

Figure 8. Comparison of *n*-octane vapor pressure data with available literature values

Table V. Parameters of Helium Molar Flowrate

Variable	Uncertainty	Relative uncertainty, %
P	±0.01 inch Hg	±0.0327
T	±0.03K	±0.0098
V	±0.0001 inch (diameter) ±0.001 inch/foot (screw)	±0.0184
B_{He}	11.80 ± 0.121 cc/mol at 305K	±1.026

cally dependent upon measurement precision and equipment limitations.

In the design of the experimental program, it was recognized that uncertainties in the gas-analysis equipment would probably determine the limit of accuracy. It was not anticipated, however, that the uncertainty would be as great as it actually was. The preliminary calibration of this and other equipment was well worth the time in pinpointing possible areas of malfunction. Based upon calibration results, assessments of various systematic uncertainties are given below.

Molar flow rate of the helium carrier gas is determined from the variables in Table V. This results in a relative uncertainty in compressibility factor of 0.0012%, or, the overall relative uncertainty in carrier gas flowrate is less than 0.07%.

Several considerations determine the micropump flowrate. In the case of liquid metering, API 44 gives uncertainties in reported liquid density values of 0.022 to 0.0002 g/cm^3 in density. However, since pumping temperature was about 32°C, where the reported densities should be rather accurate, the uncertainty was taken to be ±0.0002 g/cm^3. The uncertainty in the micropump temperature is ±0.1°C. Hence, the overall systematic uncertainty in density is ±0.0003 g/cm^3 or a relative uncertainty of about 0.0488%. Using the tolerance on the metering screw and plunger diameter gives an over-all uncertainty in molar flowrate of less than 0.1% when metering liquids.

For vapor metering, the uncertainties in the second virial coefficient at 32°C by Dymond and Smith (*18*) are given in Table VI. This results in an overall systematic uncertainty less than 0.18% in the molar flowrate.

The maximum uncertainty in the equilibrium cell temperature is ±0.025°C, composed of a maximum temperature fluctuation of ±0.015°C and a difference between the practical temperature scale and the absolute scale of ±0.01°C. Uncertainty in the measured cell pressure was ±0.01 in. of Hg. Relative uncertainties for temperature were then ±0.025 to ±0.075%. Relative uncertainty in pressure ranged from ±0.033 to ±0.011%.

Limit on the gas-phase analysis is determined by the following considerations. Since this investigation required accurate measurement of absolute currents over wide ranges, it was necessary to be sure that the attenuator and sensitivity scales were self-consistent over wide ranges. The calibration procedure indicated that the analysis equipment was self-consistent to within 2–3% after use of a nonlinearity correction factor derived from a mass of calibration data. This was considered adequate, as the manufacturer's original specifications called for only 1% linearity on the attenuator and a corresponding tolerance on the sensitivity scales. Thus, from the calibration data the uncertainty of any current determination was 2–3%. Calibration data were fitted to an average deviation of less than 2% with a maximum deviation of 4–5%. Most of the partial pressure vs. total pressure data were fitted to less than 1% deviation by the model used, which gives an indication of the internal consistency of

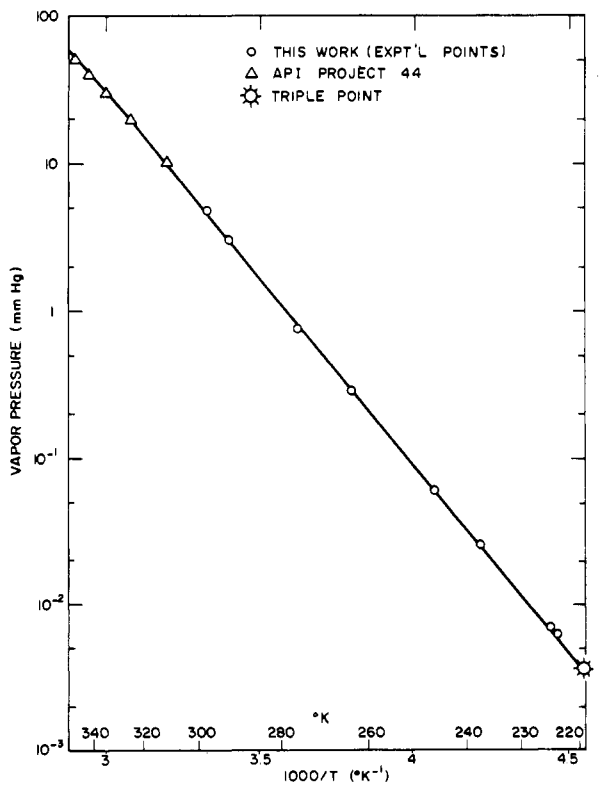

Figure 9. Comparison of *n*-nonane vapor pressure data with available literature values

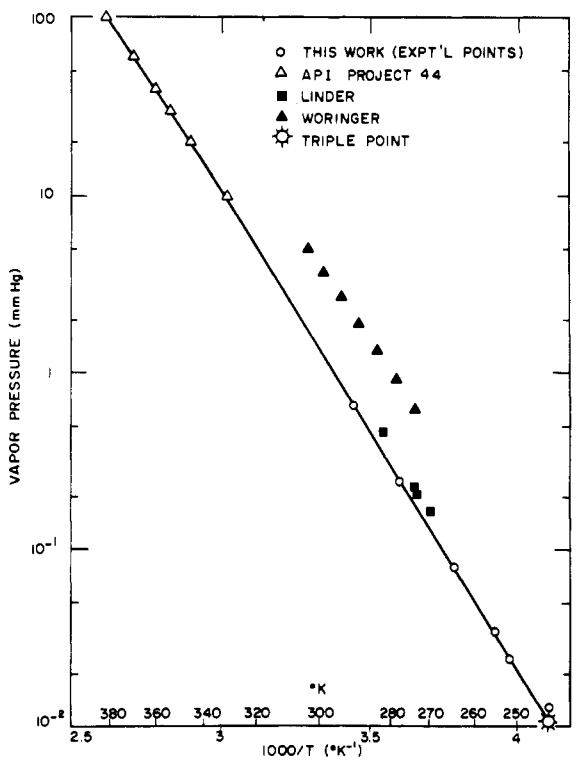

Figure 10. Comparison of *n*-decane vapor pressure data with available literature values

Table VI. Variables in Vapor Metering

Compound	Second virial coeff, cc/mol	Rel. uncertainty, %
Ethane	−177 ± .	±2.825
Propane	−367 ± 13.7	±3.733
n-Butane	−69o ± .0	±2.874

Using maximum uncertainty in B (propane), we have:

Variable	Uncertainty	Rel. uncertainty, %
T	±0.1°C	±0.0328
V	±0.0001 inch (diameter) ±0.001 inch/foot (screw)	±0.0534
P	±0.01 inch Hg	±0.0312
Z	±0.00059 (based on C_3)	±0.0598

the experimental points at a given temperature. The average deviations of the experimental data from the Clausius-Clapeyron smoothing equation average less than 3%. Consequently, it is concluded that the experimental vapor pressure measurements are accurate to within 3%. The bulk of the uncertainty can be assigned to the electronic measurements of the detector signal.

Acknowledgment

Donation of the high purity hydrocarbons used in this investigation by the Phillips Petroleum Co. is sincerely appreciated. The assistance of Patsy S. Chappelear in the preparation of this manuscript is gratefully acknowledged.

Nomenclature

A, B = parameters for vapor pressure equations
B_{ij} = second virial coefficient, $cm^3/g\text{-mole}$
C_{ijk} = third virial coefficient, $(cm^3/g\text{-mole})^2$
f_i^v, f_i^c = fugacity of component i in vapor or condensed phase
f_2^{0c} = standard state fugacity—(i.e., fugacity of pure condensed 2 at temperature T adjusted to zero pressure
FID = flame ionization detector
H = enthalpy, cal/g-mol
ΔH_v = enthalpy of vaporization, cal/g-mol
ΔH_f, ΔH_m = enthalpy of fusion or melting, cal/g-mol
$n\text{-}C_j$ = normal paraffin having J carbon atoms
n_i = moles of component i
P = pressure, mm Hg absolute, or atmospheres
PRT = platinum resistance thermometer
P_c = critical pressure, atmospheres
P_i^s = saturated vapor pressure of pure condensed i, mm Hg
P_t = triple point pressure, mm Hg
P_r = reduced pressure, P/P_c
R = gas constant or electrical resistance, as indicated by context
S = entropy, cal/g-mol-K
T = temperature, K or °C
T_b = temperature of normal boiling point, K or °C
T_c = Critical temperature, K or °C
T_f = freezing point temperature, K or °C
T_r = reduced temperature, T/T_c
T_t = triple point temperature, K or °C
V = volume, cc or liters
V_i^c, V_i^l, V_i^s = molar volumes for phases characterized as condensed, liquid, or saturated vapor, respectively, cc or liter (for component i)
V_c = critical volume, cm^3 or liters
$\bar{V}_i$ = partial molar volume of component i
x_i = mole fraction in liquid phase for i
Y_i = mole fraction of i in vapor phase
Z = compressibility factor, PV/RT

Greek Letters

γ_i = liquid phase activity coefficient for component i at temperature T, adjusted to zero pressure
ϕ_i^v, ϕ_i^c = fugacity coefficient for component i in vapor or condensed phase
ϵ = enhancement factor, Py/P^s

Literature Cited

(1) Adam, H., Ed., "1965 Transactions of Third International Vacuum Congress," Vol. 1, Pergamon Press, New York, 1966.
(2) Altschuller, A. P., Cohen, I. R., *Anal. Chem.*, **32**, 802 (1960).
(3) Beattie, J., *Chem. Rev.*, **44**, 141 (1949).
(4) Bell, G. H., Groszek, A. J., *J. Inst. Petrol.*, **48**, 325 (1962).
(5) Carruth, G. F., Ph.D. thesis, Rice University, Houston, Tex., 1970.
(6) Carruth, G. F., Kobayashi, Riki, *Anal. Chem.*, **44**, 7 (1972).
(7) Carruth, G. F., Kobayashi, Riki, *Ind. Eng. Chem. Fundamentals*, **11**, 509 (1972).
(8) Chang, H. L., Ph.D. thesis, Rice University, Houston, Tex., 1966.
(9) Chao, K. C., Greenkorn, R. A., Olabisi, O., Hensel, B. H., 66th National Meeting, A.I.Ch.E., Portland, Ore. Aug. 24–27, 1969.
(10) Chapman, S., Cowling, T. G. "The Mathematical Theory of Non-uniform Gases," 3rd ed., Cambridge University Press, Cambridge, 1970.
(11) Chiu, C., Canfield, F. B., *Adv. Cryog. Eng.*, **12**, 741 (1967).
(12) Condon, R. D., Scholly, P. R., Averill, W., "Comparative Data on Two Ionization Detectors," in "Gas Chromatography 1960," Butterworths, Washington, 1960.
(13) Delaplace, R., *Compt. Rend.*, **204**, 493 (1937).
(14) Desty, D. H., Geach, C. J., Goldup, A., "Examination of the Flame Ionization Detector Using a Diffusion Dilution Apparatus," in "Gas Chromatography 1960," Butterworths, Washington, 1960.
(15) Dokoupil, Z., Van Soest, G., Swenker, M. D. P., *Appl. Sci. Res.*, **A5**, 182 (1955).
(16) Drucker, C., Jimeno, E., Kangro, W., *Z. Phys. Chem.*, **90**, 513 (1915).
(17) Dushman, S., "Scientific Foundations of Vacuum Technique," Wiley, New York, N.Y., 1949.
(18) Dymond, J. H., Smith, E. B., "Virial Coefficients of Gases," Oxford University Press, Oxford, 1969.
(19) Ewald, A. H., *Trans. Faraday Soc.*, **51**, 347 (1955).
(20) Ewald, A. H., Jepson, W. B., Rowlinson, J. S., *Discussions Faraday Soc.*, **15**, 238 (1953).
(21) Francis, M., *Trans. Faraday Soc.*, **31**, 1325 (1935).
(22) Gerry, H. T., Gillespie, L. J., *Phys. Rev.*, **40**, 269 (1932).
(23) Gill, J. M., Hartman, C. H., *J. Gas Chromatogr.*, **5**, 605 (1967).
(24) Hála, E., Pick, J., Fried, V., Vilim, O., "Vapour-Liquid Equilibrium," 2nd ed., Pergamon Press, New York, N.Y., 1967.
(25) Heck, C. K., Ph.D. dissertation, University of Colorado, 1968.
(26) Hickman, K. C. D., *J. Opt. Soc. Amer.*, **18**, 305 (1929).
(27) Hirschfelder, J. O., Curtiss, C. F., Bird, R. B., "Molecular Theory of Gases and Liquids," Wiley, New York, 1964.
(28) Hiza, M. J., Duncan, A. G., *AIChE J.*, **16**, 733 (1970).
(29) King, W. H., Jr., DuPre, G. C., *Anal. Chem.* **41**, 1936 (1969).
(30) Kirk, B. S., Ziegler, W. T., Mullins, J. C., *Adv. Cryog. Eng.*, **6**, 413 (1961).
(31) Knudsen, M., *Ann. Phys.*, **28**, 999 (1909).
(32) Knudsen, M., *ibid.*, **32**, 809 (1910).
(33) Lannung, A., *J. Amer. Chem. Soc.*, **52**, 68 (1930).
(34) Leland, T. W., Jr., Chappelear, P. S., *Ind. Eng. Chem.*, **60**(7), 15 (1968).
(35) Lewin, G., "Fundamentals of Vacuum Science and Technology," McGraw-Hill, New York, N.Y., 1965.
(36) Lewis, G. N., Randall, M., "Thermodynamics" (rev. by K. S. Pitzer and L. Brewer), 2nd ed., McGraw-Hill, New York, N.Y., 1961.
(37) Liang, S. C., *J. Appl. Phys.*, **22**, 148 (1951).
(38) Liang, S. C., *J. Phys. Chem.*, **56**, 660 (1952).
(39) Linder, E. G., *ibid.*, **35**, 531 (1931).
(40) Lovelock, J. E., *Anal. Chem.*, **33**, 162 (1961).
(41) Lynch, E. J., Wilke, C. R., *J. Chem. Eng. Data*, **5**, 300 (1960).
(42) Markham, A. E., Kobe, K. E., *Chem. Rev.*, **28**, 519 (1941).
(43) McNair, H. M., Bonelli, E. J., "Basic Gas Chromatography," Varian Aerograph, Walnut Creek, Calif., 1967.
(44) Messerley, G. H., Kennedy, R. M., *J. Amer. Chem. Soc.*, **62**, 2988 (1940).
(45) Mikkelson, L., *J. Gas Chromatogr.*, **5**, 601 (1967).
(46) Mündel, C. F., *Z. Phys. Chem.*, **85**, 435 (1913).
(47) Nesmeyanov, An. N., "Vapour Pressure of the Elements," Academic Press, New York, 1963.
(48) Parks, G. S., Moore, G. E., *J. Chem. Phys.*, **17**, 1151 (1949).
(49) Partington, J. R., "Advanced Treatise on Physical Chemistry," Vol. 2, Longmans, Green, New York, N.Y., 1951.

(50) Patterson, G. N., "Molecular Flow of Gases," Wiley, New York, N.Y., 1956.
(51) Pitzer, K. S., Curl, R. F., Jr., "Thermodynamic Properties of Normal Fluids," Conference on Thermodynamics and Transport Properties of Fluids, Institution of Mechanical Engineers, London, July 10–12, 1956.
(52) Pitzer, K. S., Curl, R. F., Jr., *J. Amer. Chem. Soc.*, **79**, 2369 (1957).
(53) Pitzer, K. S., Lippmann, D. Z., Curl, R. F., Jr., Huggins, C. M., Petersen, D. E., *ibid.*, **77**, 3433 (1955).
(54) Prausnitz, J. M., Chueh, P. L., "Computer Calculations for High-Pressure Vapor-Liquid Equilibria," Prentice-Hall, Englewood Cliffs, N.J., 1968.
(55) Prausnitz, J. M., Eckert, C. A., Orye, R. V., O'Connell, J. P., "Computer Calculations for Multicomponent Vapor-Liquid Equilibria," Prentice-Hall, Englewood Cliffs, N.J., 1967.
(56) Prausnitz, J. M., "Molecular Thermodynamics of Fluid-Phase Equilibria," Prentice-Hall, Englewood Cliffs, N.J., 1969.
(57) Regnault, V., *Ann. Chim. Phys.*, **15**, Ser. 3, 129 (1845).
(58) Reid, R. C., Sherwood, T. K., "Properties of Gases and Liquids," 2nd ed., McGraw-Hill, New York, N.Y., 1966.
(59) Reuss, J., Beenakker, J. J. M., *Physica*, **22**, 869 (1956).
(60) Robin, S., Vodar, B., *Discussions Far. Soc.*, **15**, 233 (1953).
(61) Rossini, F. D., Pitzer, K. S., Arnett, R. L., Brann, R. M., Pimentel, G. C., "Selected Values of Physical and Thermodynamic Properties of Hydrocarbons and Related Compounds," Am. Petrol. Inst. Project 44, Carnegie Press, Pittsburgh, Pa., 1953.
(62) Ruska, W. E. A., Carruth, G. F., Kobayashi, Riki, *Rev. Sci. Instrum.*, **43**, 1331 (1972).
(63) Schindler, D. L., Ph.D. Thesis, University of Kansas, Lawrence, Kan., 1966.
(64) Sinor, J. E., Ph.D. Thesis, University of Kansas, Lawrence, Kan., 1965.
(65) Smith, G. E., Sonntag, R. E., Van Wylen, G. J., *Adv. Cryog. Eng.*, **8**, 162 (1963).
(66) Steinherz, H. A., "Handbook of High Vacuum Engineering," Reinhold, New York, N.Y., 1963.
(67) Stephen, H., Stephen, T. "Solubilities of Inorganic and Organic Compounds," Macmillian, New York, N.Y., 1963.
(68) Stull, D. R., *Ind. Eng. Chem.*, **39**, 517 (1947).
(69) Tickner, A. W., Lossing, F. P., *J. Chem. Phys.*, **18**, 148 (1950).
(70) Tickner, A. W., Lossing, F. P., *J. Phys. Colloid Chem.*, **55**, 733 (1951).
(71) Timmermans, J., "Physico-Chemical Constants of Pure Organic Compounds," p. 84, 660, Elsevier, New York, N.Y., 1950.
(72) Weast, R. C., Ed., "Handbook of Chemistry and Physics," 49th ed, Chemical Rubber Co., Cleveland, Ohio, 1968.
(73) Weissberger, A., Ed., "Physical Methods of Organic Chemistry," Vol. 1, Interscience, New York, N.Y., 1959.
(74) Wichterle, I., Monograph, Rice University, Houston, Tex., 1970.
(75) Woringer, B., *Z. Phys. Chem.*, **34**, 257 (1900).
(76) Ziegler, W. T., Kirk, B. S., Mullins, J. C., Berquist, A. R., "Calculation of the Vapor Pressure and Heats of Vaporization and Sublimation of Liquids and Solids Below One Atmosphere Pressure. VII. Ethane," Techn. Rept. 2, Project A-764 Engineering Experiment Station, Georgia Institute of Technology, Dec. 31, 1964 (Contract CST-1154, National Bureau of Standards, Washington, D.C.).
(77) Ziegler, W. T., Mullins, J. C., Kirk, B. S., "Calculation of the Vapor Pressure and Heats of Vaporization and Sublimation of Liquids and Solids, Especially Below One Atmosphere Pressure. I. Ethylene," Tech. Rept. 1, Project A-460, Engineering Experiment Station, Georgia Institute of Technology, June 2, 1962 (Contract CST-7238, National Bureau of Standards, Boulder, Colo.).
(78) Ziegler, W. T., Mullins, J. C., Kirk, B. S. "Calculation of the Vapor Pressure and Heats of Vaporization and Sublimation of Liquids and Solids, Especially below One Atmosphere Pressure. III. Methane," Tech. Rept. 3, Project A-460, Engineering Experiment Station, Georgia Institute of Technology, Aug. 31, 1962 (Contract CST-7238, National Bureau of Standards, Boulder, Colo.).

Received for review June 12, 1972. Accepted November 10, 1972. A NDEA Fellowship by the Office of Education and supplementary financial support by the National Science Foundation, Rice University, and the Monsanto Co. for G. F. Carruth are gratefully acknowledged.

Vapor Pressure and Sublimation Enthalpy of Anthraquinone and of 1,5- and 1,8-Dihydroxyanthraquinones

Giampiero Bardi, Rosario Gigli, Leopoldo Malaspina and Vincenzo Piacente
Laboratorio di Chimica Fisica ed Elettrochimica, Istituto Chimico Università di Roma, Roma, Italy

The vapor pressure and the sublimation enthalpy of anthraquinone have been simultaneously determined by a microcalorimetric Knudsen effusion technique, utilizing a Calvet differential microcalorimeter:

$$\log p_{torr} = (11.94 \pm 0.08) - (5624 \pm 32)/T$$

$$\Delta H_{sub}^{\circ}(T) = (30007 \pm 106) - (10.01 \pm 0.24)T \text{ cal mol}^{-1}$$

The vapor pressure of the derivatives 1,5- and 1,8-dihydroxyanthraquinones has been determined, measuring the rates of mass loss in the Knudsen conditions, utilizing a SETARAM model B-60 Ugine Eyraud thermobalance:

1,5-dihydroxy anthraquinone: $\log p_{torr} = (12.90 \pm 0.09) - (6435 \pm 38)/T$

1,8-dihydroxy anthraquinone: $\log p_{torr} = (13.14 \pm 0.06) - (6098 \pm 26)/T$

The Gibbs energy functions of condensed anthraquinone have also been estimated.

Very few sets of vapor pressure and sublimation enthalpy data of anthraquinone and its 1,5- and 1,8-dihydroxy derivatives are reported in the literature. Hoyer and Peperle *(5)* determined the vapor pressure–temperature dependence for these substances by an effusion method, and Beynon and Nicholson *(2)* measured the sublimation enthalpy of these compounds by means of a radioactive ionization gage.

Previously, vapor pressure determinations for the anthraquinone were carried out by Inokuchi and Coll *(6)* and, in a range of higher pressures (>100 torr), by Nelson and Senseman *(13)*, utilizing the effusion and manometric methods, respectively. As for the sublimation enthalpy of the anthraquinone, only the value proposed by Magnus *(7)* and that recently determined by Beech and Lintonbon *(1)* with a scanning differential calorimeter are available.

The not very good agreement of the reported data led us to effect new determinations of the vapor pressure and sublimation enthalpy of these three compounds. Study of the anthraquinone was based on the differential calorimetry combined with the Knudsen effusion technique for simultaneous determinations of vapor pressures and sublimation enthalpies of the same sample *(8–10)*.

Due to the relative temperature ranges (too high for the employment of the apparatus used for anthraquinone), vapor pressures of the two derivatives, 1,5- and 1,8-dihydroxyanthraquinone, were determined by a thermobalance measuring the rate of mass loss in the Knudsen conditions.

Experimental and Results

Anthraquinone. The microcalorimetric measurements were made with a SETARAM Calvet differential microcalorimeter described elsewhere *(3, 11)*. The twin microcalorimeter elements were placed symmetrically in a Kanthal block, and the differential thermal flow was measured by two thermopiles in opposition, 396 Pt and Pt-Rh 10% thermocouples, connected with a galvanometer. The thermogram was a recording guided by the same galvanometer. The assembly and evaporation experiment were described in detail in previous works *(8–10)*.